Accurate many-body calculations on the lowest ^2S and ^2P states of the lithium atom

Ingvar Lindgren
Department of Physics, Chalmers University of Technology and the University of Gothenburg, S-41296 Göteborg, Sweden
(Received 25 July 1984)

The many-body perturbation theory (MBPT) in the coupled-cluster formulation is applied to perform very accurate calculations on the 2^2S and 2^2P states of the lithium atom. The computational procedure is based on coupled one- and two-particle equations, which are solved iteratively. In this way it has been possible to evaluate almost all one- and two-particle effects—i.e., the core polarization and the pair correlation—to essentially all orders of perturbation theory. The main reasons for this work are to test the computational procedure and to determine the significance of genuine three-particle effects, which are not included in the calculation. The total energy, the valence electron binding energies, and the hyperfine-interaction parameters are calculated for the two states. The perturbation effect, i.e., the difference between the experimental value and the Hartree-Fock result, is in all cases reproduced within about 1%, except for the small hyperfine parameter of the $2^2P_{3/2}$ state, where this discrepancy is about 4%, mainly due to some remaining error in the induced contact interaction. The quadrupole parameter of the $2^2P_{3/2}$ state is expected to be accurate to a few tenths of a percent. No improved value of the quadrupole moment can be given, however, due to experimental uncertainty.

I. INTRODUCTION

During the last decades several procedures have been developed for accurate atomic and molecular calculations. One of the most powerful and most frequently used procedures is the many-body perturbation theory (MBPT), based on the original works of Brueckner[1] and Goldstone[2] and first applied to atomic calculations by Kelly.[3] This procedure, first adapted to closed-shell and other single-determinantal states, has later been extended to general open-shell systems by Brandow,[4] Sandars,[5] Lindgren,[6] and others,[7,8] and a comprehensive treatment of this procedure can be found in the recent monograph by Lindgren and Morrison.[9]

In our research group at Chalmers University of Technology we have developed a number of routines for atomic MBPT calculations, primarily for hyperfine-structure investigations,[10–12] but subsequently applied also to fine-structure splittings,[13,14] correlation energies and term splittings,[15,16] isotopic shifts,[17,18] and parity nonconservation.[19,20]

Our computational procedure is based upon the use of coupled, inhomogeneous one- and two-particle equations, which are solved in an iterative way. It is then possible to include core-polarization and pair-correlation effects essentially to all orders of perturbation theory. This procedure has been tested on He-like systems—where it would be virtually exact—and there found to yield very accurate results.[15,18] It is the purpose of the present work to perform an accurate test of this procedure on the lithium atom, which is a three-electron system. The correlation energy, ionization energy, and hyperfine structure are calculated for the lowest ^2S and ^2P states, and the results are compared with those of other accurate calculations as well as with available experimental data. Similar calculations on heavier atoms are now under way in our group and will be published separately.

The main purpose of this series of works is to find out to what extent this procedure, when pushed to its limit, is capable of producing the complete polarization and pair-correlation effects and to what extent these effects represent the entire perturbation of an atomic system. A particularly interesting question is how important "genuine" three-particle effects are, i.e., three-body effects that cannot be included in a pair-correlation procedure. It should be noted that large groups of effects, which are normally classified as "three-body effects," are, in fact, included in the procedure that we employ. In addition, the most important four-particle correlations are included by means of the so-called coupled-cluster procedure, as will be briefly described below.

Our procedure is most developed for atoms with a single valence electron, like the alkali-metal atoms, and the most advanced tests will be performed for such systems. For atoms with several valence electrons new effects appear, which so far are only partially included in our procedure,[21] and here further developments are needed before we have reached the same level of accuracy as for systems with a single valence electron.

II. THEORY

The formalism underlying our computational procedure has been described in detail in the literature,[9,12] but for the convenience of the reader we shall give a summary here as a basis for the following treatment.

A. Basic formalism

The atomic Hamiltonian

$$H=-\tfrac{1}{2}\sum_{n=1}^{N}\nabla_n^2-\sum_{n=1}^{N}\frac{Z}{r_n}+\sum_{n=1}^{N}\sum_{\substack{m=1\\m<n}}\frac{1}{r_{mn}} \tag{1}$$

using atomic units and conventional notations, is partitioned in the usual way into an unperturbed Hamiltonian

$$H_0=\sum_{n=1}^{N}\left[-\tfrac{1}{2}\nabla_n^2-\frac{Z}{r_n}+U(r_n)\right]=\sum_{n=1}^{N}h_0(n) \tag{2}$$

and a perturbation

$$V=H-H_0=\sum_{n=1}^{N}\sum_{\substack{m=1\\m<n}}\frac{1}{r_{mn}}-\sum_{n=1}^{N}U(r_n)\,. \tag{3}$$

The unperturbed Hamiltonian (2) is here assumed to be of central-field type with a spherically symmetric potential $U(r)$. The single-particle equation

$$h_0\varphi_i=\epsilon_i\varphi_i \tag{4}$$

defines a set of electron orbitals, which form the basis of the calculation. The Slater determinants ϕ^A formed by these orbitals are antisymmetrized eigenfunctions of H_0

$$H_0\phi^A=E_0^A\phi^A \tag{5}$$

with the eigenvalue equal to the sum of the orbital eigenvalues of the determinant

$$E_0^A=\sum_i\epsilon_i\quad(\varphi_i\in\phi^A)\,. \tag{6}$$

We separate the functional space into a *"model space"* (P), spanned by the eigenfunctions associated with one or several eigenvalues of H_0 (configurations), and a *complementary space* (Q). The full wave functions, which have their major parts within the model space, can then be expressed

$$\Psi^a=\Omega\Psi_0^a\quad(a=1,2,\ldots,d) \tag{7}$$

where the zeroth-order wave function Ψ_0^a is the projection of the full wave function onto the model space,

$$\Psi_0^a=P\Psi^a\,, \tag{8}$$

and d is the dimensionality of this space. It can be shown that the *wave operator* Ω satisfies a *"generalized Bloch equation"*[6,9,22,23]

$$[\Omega,H_0]P=Q(V\Omega-\Omega PV\Omega)P \tag{9}$$

which can be conveniently used to generate a perturbation expansion of this operator.

Using the *intermediate normalization*

$$\langle\Psi_0^a\,|\,\Psi^a\rangle=\langle\Psi_0^a\,|\,\Psi_0^a\rangle=1 \tag{10}$$

we can expand the wave operator in the following way:

$$\Omega=1+\Omega^{(1)}+\Omega^{(2)}+\cdots\,. \tag{11}$$

Inserting this expansion into (9) and identifying terms of the same order, we obtain the Rayleigh-Schrödinger expansion[6,9]

$$\begin{aligned}&[\Omega^{(1)},H_0]P=QVP\,,\\&[\Omega^{(2)},H_0]P=Q(V\Omega^{(1)}-\Omega^{(1)}PV)P\,,\\&[\Omega^{(3)},H_0]P=Q(V\Omega^{(2)}-\Omega^{(2)}PV-\Omega^{(1)}PV\Omega^{(1)})P\,,\end{aligned} \tag{12}$$

and so on. This expansion forms the basis for the MBPT formalism that we employ.

By projecting the Schrödinger equation

$$H\Psi^a=E^a\Psi^a\quad(a=1,2,\ldots,d) \tag{13}$$

onto the model space, we obtain, using Eqs. (7) and (8),

$$PH\Omega\Psi_0^a=E^a\Psi_0^a\,. \tag{14}$$

The operator

$$H_{\text{eff}}=PH\Omega P \tag{15}$$

is called the *effective Hamiltonian,* and it has the zeroth-order wave functions Ψ_0^a as eigenfunctions and the corresponding *exact* energies as eigenvalues. Since the zeroth-order wave functions are assumed to be normalized, (10), we can express the exact energies as

$$E^a=\langle\Psi_0^a\,|\,H_{\text{eff}}\,|\,\Psi_0^a\rangle\,. \tag{16}$$

If we consider an additional perturbation h, like the hyperfine interaction, then we make the formal replacement

$$H\rightarrow H+h \tag{17}$$

in the perturbation expansion, which leads to

$$H_{\text{eff}}\rightarrow H_{\text{eff}}+h_{\text{eff}}\,. \tag{18}$$

Here, the operator h_{eff} contains all parts of the effective Hamiltonian which depend on the additional perturbation h. The corresponding energy contribution is then

$$\Delta E_h^a=\langle\Psi_0^a\,|\,h_{\text{eff}}\,|\,\Psi_0^a\rangle\,. \tag{19}$$

The operator h_{eff} is called the *"effective operator"* corresponding to the additional perturbation h. This is the quantity evaluated in our hyperfine investigation.

B. Graphical representation

In order to generate a graphical representation of the wave operator [Eqs. (11) and (12)] in terms of Goldstone-like diagrams,[2–4] we express the perturbation (3) and the wave operator in second quantization:

$$\begin{aligned}V&=\sum_{i,j}a_i^\dagger a_j\langle i\,|\,(-U)\,|\,j\rangle\\&\quad+\tfrac{1}{2}\sum_{i,j,k,l}a_i^\dagger a_j^\dagger a_l a_k\left\langle i,j\left|\frac{1}{r_{12}}\right|k,l\right\rangle\,,\\\Omega&=1+\sum_{i,j}a_i^\dagger a_j x_i^j+\tfrac{1}{2}\sum_{i,j,k,l}a_i^\dagger a_j^\dagger a_l a_k x_{ij}^{kl}+\cdots\end{aligned} \tag{20}$$

and similarly for the individual terms in the order-by-order expansion

$$\Omega^{(m)}=\sum_{i,j}a_i^\dagger a_j x_i^{(m)j}+\cdots\,. \tag{21}$$

Here, the operators are in *normal form with respect to the vacuum,* i.e., with the creation operators to the left of the annihilation operators. In atomic and molecular calculations it is usually more convenient to work in the so-called *particle-hole* (p-h) *formalism,* which implies that the operators are normal ordered with respect to some suit-

able (closed-shell) *reference state* (Φ_0). The operators (20) can then be separated into normal-ordered zero-, one-, two-, . . . body operators in the following way:[9,23–25]

$$V = V_0 + V_1 + V_2 ,$$

$$V_0 = \langle \Phi_0 | V | \Phi_0 \rangle = \sum_a^{\text{hole}} \langle a | (-U) | a \rangle + \tfrac{1}{2} \sum_{a,b}^{\text{hole}} \left\langle a,b \left| \frac{\tilde{1}}{r_{12}} \right| a,b \right\rangle ,$$

$$V_1 = \sum_{i,j} \{a_i^\dagger a_j\} \langle i | v | j \rangle = \sum_{i,j} \{a_i^\dagger a_j\} \left[\langle i | (-U) | j \rangle + \sum_a^{\text{hole}} \left\langle i,a \left| \frac{\tilde{1}}{r_{12}} \right| j,a \right\rangle \right] , \tag{22}$$

$$V_2 = \tfrac{1}{2} \sum_{i,j,k,l} \{a_i^\dagger a_j^\dagger a_l a_k\} \left\langle i,j \left| \frac{1}{r_{12}} \right| k,l \right\rangle ,$$

$$\Omega = 1 + \sum_{i,j} \{a_i^\dagger a_j\} x_i^j + \tfrac{1}{2} \sum_{i,j,k,l} \{a_i^\dagger a_j^\dagger a_l a_k\} x_{ij}^{kl} + \cdots$$

and similarly for the expansion (21). Here, the curly brackets are used to denote the normal ordering with respect to the reference state. The orbitals a and b run over hole states, i.e., orbitals occupied in the reference state, while i,j,k,l run over *all* orbitals—particle as well as hole states. The tilda over $1/r_{12}$ indicates that the *exchange* integral is included.[26]

With the form (22) of V and Ω and Wick's theorem for normal-ordered operators[9]

$$AB = \{AB\} + \{\overline{AB}\} \tag{23}$$

the right-hand sides (rhs) of the Rayleigh-Schrödinger expansion (12) can be expressed in normal form, and identification with the left-hand side (lhs)—simply supplying an energy denominator—then yields an order-by-order expansion of the wave operator in second quantization. The term $\{\overline{AB}\}$ in (23) represents all possible single, double, . . . *contractions* between the p-h annihilation operators of A and the p-h creation operators of B, while $\{AB\}$ represents the normal form of AB without any contractions.

In the graphical representation *particles* are denoted by lines directed *upwards* and *holes* by lines directed *downwards* (see Fig. 1), and the normal form of the perturbation (22) can then be represented as shown in Fig. 2. Wick's theorem (23) is in this graphical representation applied simply by joining the lines at the bottom of A with those at the top of B in all possible ways.[9] Each joint (contraction) gives rise to a diagram. A straightforward application of this procedure leads to a diagrammatic expansion of the wave operator, and the diagrams can then be evaluated according to standard rules.[9]

In our general open-shell procedure—following Brandow[4] and Sandars[5]—we shall furthermore separate the orbitals into *three* categories, (a) *core* orbitals, which are occupied in *all* determinants of the model space, (b) *valence* orbitals, which are occupied in *some* and (c) *virtual* orbitals, which are *not* occupied in *any* determinant of the model space. In principle, the valence orbitals can be of particle *or* hole type, but we shall assume here that they are all *particles*. The core orbitals must be of hole type, and this means that in this application core and hole states are identical. This implies that *our reference state is a determinant with all core orbitals occupied.* Graphically we represent the valence orbitals with double arrows—directed upwards, since they are particles (see Fig. 1).

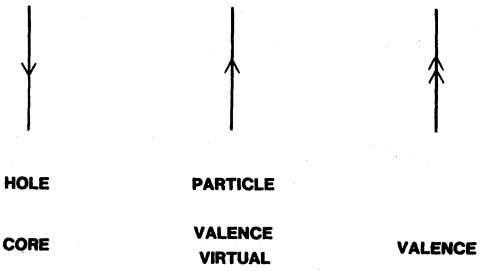

FIG. 1. Graphical representation of different kinds of electron orbitals. Note that a line with a *single* arrow directed upwards represents a general particle state, i.e., a valence *or* a virtual state, while a line with a *double* arrow is used to represent valence states only.

We also assume that the model space is *complete,* in the sense that it contains all determinants that can be formed by distributing the valence electrons among the valence orbitals. A diagram with no other free lines than valence lines then operates within the model space and is said to be *closed.* All other diagrams operate from the model space to the complementary space and are said to be *open.*

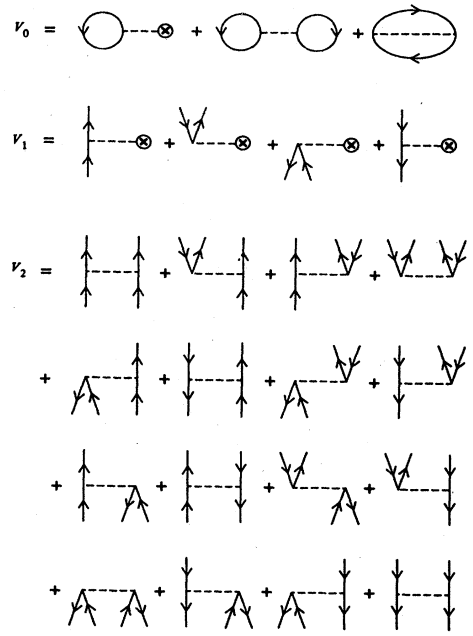

FIG. 2. Graphical representation of the electrostatic perturbation in the particle-hole formalism (22). The zero-body part V_0 is the expectation value of the perturbation in the reference state, Φ_0. The one-body part V_1 is the difference between the potential U, in the zeroth-order Hamiltonian H_0, and the Hartree-Fock potential of the reference state. If the latter is used in H_0, as in the present case, then V_1 vanishes. (From Ref. 9.)

It can then be shown that the graphical expansion of the wave operator does not contain any *unlinked* diagrams, i.e., diagrams with a *disconnected, closed part,* provided that so-called *exclusion-principle-violating* (EPV) diagrams are included. This is the general *linked-diagram theorem,*[4–9] and we can express it formally as

$$[\Omega,H_0]P=Q(V\Omega-\Omega PV\Omega)_L P\ , \tag{24}$$

where subscript L indicates that all unlinked diagrams are canceled and only linked—and EPV—diagrams have to be considered. An order-by-order expansion of this equation, in analogy with the expansion (12), yields the linked-diagram expansion

$$\begin{aligned}&[\Omega^{(1)},H_0]P=QVP\ ,\\ &[\Omega^{(2)},H_0]P=Q(V\Omega^{(1)}-\Omega^{(1)}PV)_L P\ ,\end{aligned} \tag{25}$$

and so on.

For closed-shell systems it is found that only the first term on the rhs of (12) gives rise to linked diagrams. In such a case the expansion (25) simplifies to

$$[\Omega^{(m)},H_0]P=(E_0-H_0)\Omega^{(m)}P=Q(V\Omega^{(m-1)})_L P \tag{26}$$

and the entire wave operator can be expressed by the series

$$\Omega=\sum_{m=0}^{\infty}\left[\left[\frac{Q}{E_0-H_0}V\right]^m\right]_L\ . \tag{27}$$

Such an expression is frequently used as the starting point for MBPT calculations on closed-shell systems as well as other systems with a single-determinantal unperturbed state.[3] For open-shell systems, on the other hand, the last term of Eqs. (24) and (25) does contribute and gives rise to so-called *folded*[4] or *backward*[5] diagrams.

C. The pair-correlation approach

The number of diagrams generated in the order-by-order expansion indicated above increases drastically with the order of the perturbation, and a reasonably complete calculation beyond third order is virtually prohibited in such an approach. In order to be able to get further, it is therefore more efficient to use the Bloch equation [Eqs. (9) and (24)] directly, rather than the expansions (12) and (25).

By inserting the second-quantized form of the full wave operator (22) into the Bloch equation, a set of coupled equations is obtained for the coefficients $x_i^j, x_{ij}^{kl}, \ldots$. A hierarchy of approximations can then be formed. In the first step the one-particle equations are solved, which corresponds to taking single excitations, or polarization effects, into account to all orders of perturbation theory. In the next step the coupled one- and two-particle equations are solved, which means that single and double excitations, or polarization and pair-correlation effects, are included to all orders, and so on. For practical reasons it is at present not possible to go beyond the second step in this procedure. It is reasonable to expect, however, that this step, which we refer to as the *pair-correlation approach,* should represent a good approximation to the complete solution, and it is the purpose of this and related works to test the goodness of this prediction.

For closed-shell systems the procedure described in this section is identical to the linear coupled-pair many-electron theory (CPMET) procedure of Čížek.[24,25] In the complete CPMET procedure the wave operator is expressed in exponential form

$$\Omega=\exp(S)=\sum_{n=0}^{\infty}\frac{1}{n!}S^n \tag{28}$$

which makes it possible to include important four-body effects into the two-body operator (see Fig. 12 below), and so on. This procedure is referred to as the *coupled-cluster approach,* and we shall refer to S as the *cluster operator.* In the open-shell case a similar formulation can be used, provided the operators are expressed in *normal form,* as in (22):[6,9]

$$\Omega=\{\exp(S)\}=\sum_{n=0}^{\infty}\frac{1}{n!}\{S^n\}\ . \tag{29}$$

It can be shown that the cluster operator S satisfies in the open-shell case a modified Bloch equation[6,9]

$$[S,H_0]P=Q(V\Omega-\Omega PV\Omega)_C P\ , \tag{30}$$

where subscript C indicates that only *connected* diagrams are considered. This means that the expansion of S consists in each order of connected diagrams only. The disconnected diagrams of Ω are in this formalism generated by the second and higher powers of S in the expansion (29).[27]

The cluster operator can be partitioned into one-, two-, ... body parts in the same way as the wave operator (22),

$$S=\sum_{i,j}\{a_i^\dagger a_j\}s_j^i+\tfrac{1}{2}\sum_{i,j,k,l}\{a_i^\dagger a_j^\dagger a_l a_k\}s_{kl}^{ij}+\cdots\ . \tag{31}$$

The equations for the coefficients can be obtained in the same way as the corresponding equations for the wave-operator coefficients by using (30) instead of (24).

The equations for the coefficients of the wave or cluster operators can be solved, in principle, if a "complete" set of electron orbitals (4) is available. The number of equations required will be enormous, however, if the basis set is reasonably complete.

An alternative approach, used in our applications, is to define a set of one-, two-, ... particle *functions*

$$\begin{aligned}&\eta_j=\sum_i x_j^i\varphi_i\ ,\\ &\eta_{kl}=\sum_{i,j}x_{kl}^{ij}\varphi_i\varphi_j\ ,\\ &\cdots\end{aligned} \tag{32}$$

which can be shown to satisfy corresponding inhomogeneous, differential equations. The summations extend here over all *particle* states—bound as well as unbound. For atomic systems, with spherical symmetry in zeroth order, these equations can be separated into radial and spin-angular parts, and only the former part has to be treated numerically.

The use of inhomogeneous differential equations in perturbation theory was early demonstrated by Sternheimer[28] and Dalgarno.[29] Two-particle or pair equations were first

used in MBPT calculations by Morrison,[30] using a numerical procedure developed by McKoy and Winter.[31] During the last decade these procedures have been further developed in our group at Chalmers. A polarization program, which solves the single-particle equations to all orders, was developed by Garpman *et al.*,[10] and a corresponding pair program was developed by Mårtensson-Pendrill[15] and extended to the full open-shell coupled-cluster formalism by Salomonson.[16,21] The coupling between one- and two-particle effects is treated only partially in this procedure. The most important effects of this kind, however, are taken care of by transforming the occupied orbitals into *Brueckner orbitals.*[32] A numerical procedure for doing so, using pair functions in the intermediate steps, has been developed by Lindgren *et al.*[11]

Finally, in order to evaluate the contributions to the effective operator under study [Eq. (18)], some diagram-evaluation routine is required. For the hyperfine-structure calculations the routine used by Garpman *et al.*[10] in their third-order analysis can still be used. By using iterated single-particle and pair functions instead of first-order ones—and Brueckner orbitals instead of Hartree-Fock ones—a considerable amount of higher-order effects are automatically included in this procedure. This will be considered in some detail in Sec. III.

III. NUMERICAL PROCEDURE AND RESULTS

A. Numerical procedure

The computational procedure, used in the present work to evaluate the hyperfine interaction, is indicated in Fig. 3. It contains the following main steps.

1. A self-consistent-field program (SCF) generates potential and orbitals in a *local* approximation of Hartree-Fock-Slater (HFS) type.[33] We normally use a so-called optimized Hartree-Fock-Slater (OHFS) potential[34,35]

$$U(r)=-\frac{3C}{2r}\left[\frac{3r^n\rho(r)}{4\pi^2}\right]^{1/3}, \tag{33}$$

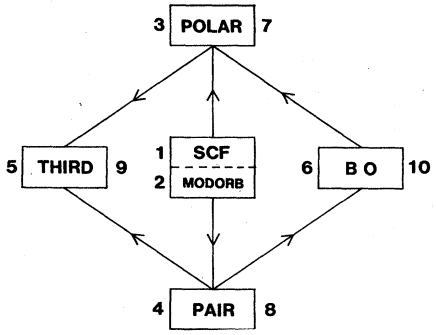

FIG. 3. Flow chart of the computational procedure used in the present work and described in the text. (SCF, self-consistent-field program with local potential; MODORB, orbital-modification routine, which generates Hartree-Fock orbitals; POLAR, iterative polarization program, which generates hyperfine and electrostatic single-particle functions; PAIR, iterative pair program, which generates pair functions; THIRD, program for evaluating third-order hyperfine diagrams; BO, routine for generating Brueckner orbitals.)

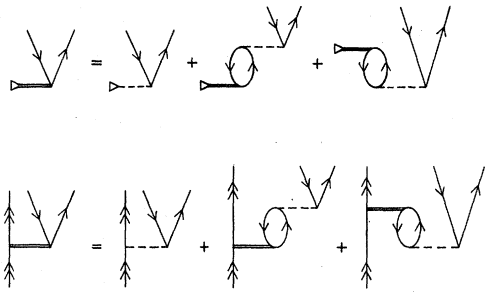

FIG. 4. Graphical representation of the single-particle equations, which are solved iteratively in the POLAR program. Top line represents the equation for hyperfine functions and the bottom line that for electrostatic functions. First diagram on the rhs represents the first-order inhomogeneous term, and the following diagrams the coupling terms, which enter in higher orders. Dotted line with a triangle represents the hyperfine interaction and the dotted line between two vertices the electron-electron interaction (as in Fig. 2). Double lines represent the "effective" interactions, obtained by solving the set of coupled equations iteratively until self-consistency. Here, as well as in all the following figures, exchange variants of the diagrams are omitted for simplicity.

where the coefficients C and n are determined by minimizing the total energy. It has been found that the combination

$$C=0.8, \quad n=1.15 \tag{34}$$

yields a good approximation for all light and medium-heavy elements ($Z \lesssim 40$). ($C=n=1$ corresponds to the original Slater approximation and $C=\alpha$, $n=1$ to the Slater $X\alpha$ potential.[36]) A local potential is used in our procedure on the lhs of the differential equations, and the nonlocal terms are treated as an inhomogeneous part on the rhs. We have then found a potential of the type of (33), (34) to be convenient and to yield good convergence in most cases.

2. The occupied (core and valence) orbitals are

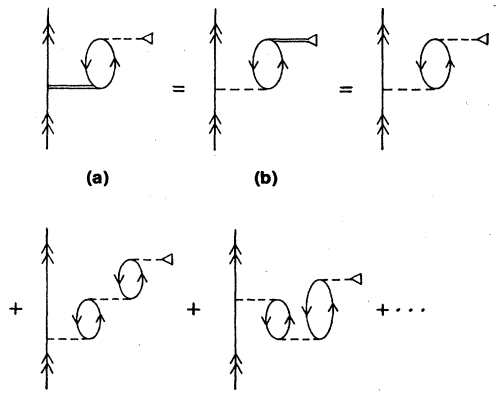

FIG. 5. Core-polarization hyperfine diagrams to all orders can be evaluated by means of iterated SPF (Fig. 4) by calculating either a hyperfine matrix element using the electrostatic SPF (a) *or* an electrostatic element using the hyperfine SPF (b).

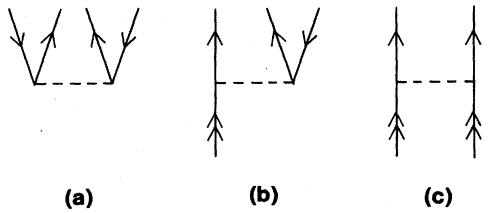

FIG. 6. Graphical representation of first-order pair functions, obtained in the pair program without iterations. (a) represents a core-core, (b) a core-valence and (c) a valence-valence excitation. For systems with only one valence electron, like the lithium atom, functions of type (c) do not appear.

transformed into Hartree-Fock (HF) orbitals by solving iteratively a single-particle equation with the "potential correction," i.e., the difference between the HF and the local potentials, as the inhomogeneous term. This orbital modification is made in a subpart (MODORB) of the polarization program (see below). In the calculations presented here we use the HF potential of the core, which has the consequence that the one-body part of the normal-ordered perturbation (22) vanishes (see Fig. 2). (In cases where the corresponding HF solution does not exist—or this procedure leads to slow convergence—the orbital-modification step can be abandoned and the potential corrections of the occupied orbitals performed iteratively, simultaneously with the corrections of the one- and two-particle functions, see point 3 below.)

3. A set of coupled single-particle equations is solved in an iterative way in the polarization program (POLAR). The perturbation can here be the hyperfine interaction *or* the electrostatic interaction with a valence electron. These equations are illustrated in Fig. 4. By means of functions of this kind the core-polarization contribution to the effective hyperfine operator (19), involving single excitations of the core, can be evaluated to all orders of perturbation theory, as illustrated in Fig. 5. The hyperfine single-particle functions (SPF), including those representing excitations from the valence shell, are stored for later use (point 5).

4. First-order pair functions are calculated in the pair program (PAIR) and stored. These functions are illustrated in Fig. 6.

5. The iterated SPF (point 3) and the first-order pair functions (point 4) are used to calculate all third-order hyperfine diagrams in a separate program (THIRD). Examples of such diagrams are shown in Fig. 7.

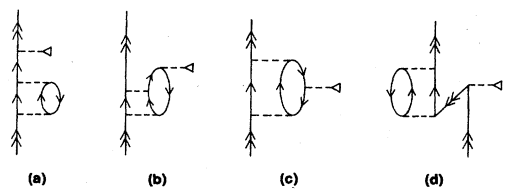

FIG. 7. Examples of third-order hyperfine diagrams, involving at least one double excitation, evaluated in the THIRD program. (a) and (b) are evaluated by means of one pair function and one hyperfine SPF, while (c) and (d) are evaluated by means of two pair functions. (d) is an example of a "folded" diagram, with a valence line running "backwards."

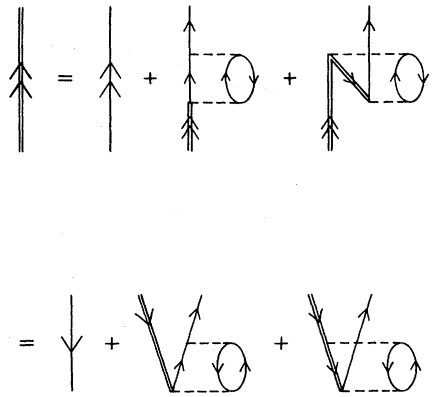

FIG. 8. Illustration of the procedure for generating approximate Brueckner orbitals (BO program); top line for a valence orbital and bottom line for a core orbital. The first diagram on the rhs represents the Hartree-Fock orbital and the following diagrams the corrections. By solving this kind of equation iteratively, also higher-order corrections are included. In our procedure, however, we iterate also the pair functions once (see Fig. 12) between each Brueckner-orbital iteration, in order to include additional pair-correlation effects into the orbitals. The use of Brueckner orbitals has the effect of eliminating explicit *single* excitations from the calculation.

6. The pair functions are used to set up right-hand sides for single-particle equations to be used for generating Brueckner orbitals. These equations are solved in a subprogram (BO) of the polarization program (POLAR), and they are illustrated in Fig. 8. The modification is most important for the valence shell. The use of Brueckner orbitals has the effect of eliminating explicit single excitations from the calculation. This means, for instance, that diagrams like that in Fig. 7(a), which has an intermediate single excitation, are included in the zeroth-order hyperfine contribution when Brueckner orbitals are used, as illustrated in Fig. 9. The right-hand side of the generating equation for the valence shell (Fig. 8, top line) can also be used to evaluate the corresponding energy correction by taking the projection on the valence orbital (see Fig. 10). This represents the lowest-order correlation contribution to the valence-electron binding energy or the

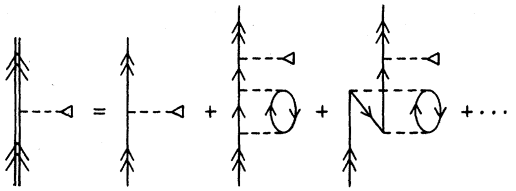

FIG. 9. By using Brueckner orbitals, important higher-order effects are automatically included in the zeroth-order hyperfine constant, as illustrated in this figure. The second diagram on the rhs is identical to the third-order diagram, shown in Fig. 7(a).

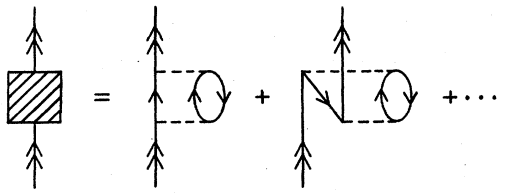

FIG. 10. From the rhs of the equation that generates approximate Brueckner orbitals for the valence shell (Fig. 8, top line), a correction to the binding energy can be obtained by taking the projection onto the valence orbital. This represents the correlation part of the ionization energy.

ionization energy.

7. The core polarization is reevaluated using Brueckner orbitals. This leads to additional contributions to the effective hyperfine operator of the type shown in Fig. 11.

8. New pair functions are generated by iterating the coupled pair equations *once* (see Fig. 12). Diagram 12(a), which represents the first-order electron-electron interaction, is evaluated using (the latest) Brueckner orbitals, and the remaining, higher-order diagrams are evaluated using the previous pair functions. Coupled-cluster diagrams, here represented by diagram 12(h), are included.

9. The "third-order" hyperfine diagrams (Fig. 7) are reevaluated, using Brueckner orbitals and iterated pair functions. This leads to additional contributions of the type illustrated in Fig. 13.

10. The process 6—9, illustrated in Figs. 8—13, is repeated. In this way a considerable number of higher-order diagrams are included in the process, a few of which are shown in Fig. 14. When this process is continued until self-consistence, practically all pair-correlation effects—including effects of single excitations—are obtained to all orders of perturbation theory.

The steps 1—5 in the process described here correspond to the procedure used by Garpman *et al.*[10(b)] and steps 1—7 to that of Lindgren *et al.*[11] More complete procedures, involving also steps 8—10, have been used previously in a few cases.[21,38,39]

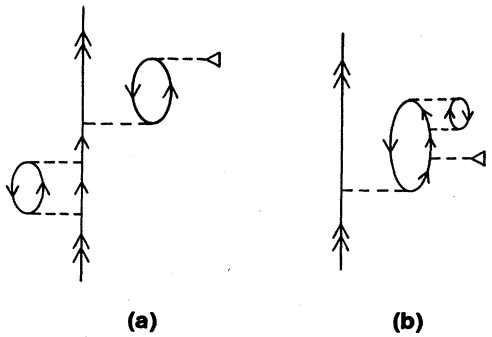

FIG. 11. Examples of fourth-order diagrams, which are included in the core polarization, when first-order Brueckner orbitals are used for the valence shell (a) and for the core (b).

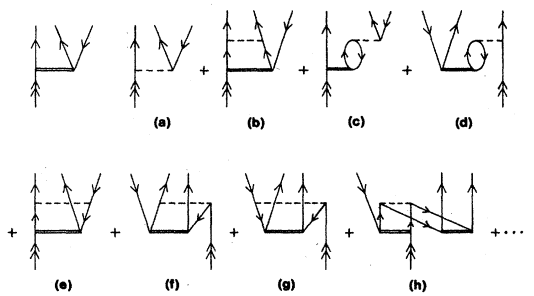

FIG. 12. The pair-correlation effect can be evaluated to all orders by solving a set of coupled pair equations iteratively, in the figure represented by an equation for a core-valence excitation. (a) is the first-order electron-electron interaction and the only nonzero term on the rhs in the first iteration. The remaining diagrams appear in the following iterations. (b)—(f) are linear terms, involving pair functions of core-valence [(b),(c),(e)] as well as core-core [(d),(f),(g)] type. (g) is an example of a nonlinear coupled-cluster diagram [see Eq. (29)], involving two pair functions. Although diagrams of this kind involve a quadrupole excitation, they can be nonzero also for two- and three-electron systems, since the exclusion principle may be violated in the linked-diagram expansion.

B. Numerical results

The choice of local potential in the self-consistent procedure is, in principle, immaterial, since the difference between this potential and the HF potential of the core is applied iteratively as a perturbation until convergence is achieved. In order to test the numerical procedure, however, we have used two different starting potentials, namely, the OHFS potential[33,34] for the neutral atom as well as of the ion with the valence electron removed, in both cases without the Latter correction.[40] (It has been found that the discontinuity introduced by this correction causes some numerical errors, which are significant on the level of accuracy aimed at here.)

In the SCF and POLAR programs we use a logarithmic

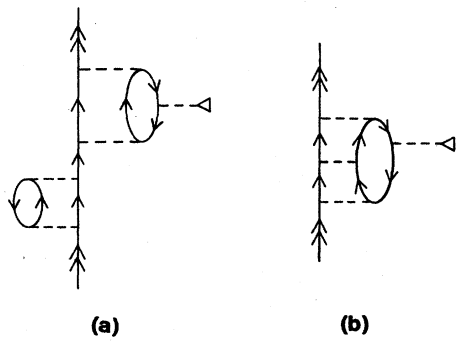

FIG. 13. Examples of higher-order hyperfine diagrams, which are included in the third-order diagrams when pair functions from the second iteration of the pair equation (Fig. 12) are used. (a) is evaluated with a first-order pair function generated with first-order Brueckner orbitals [Fig. 12(a)] and (b) with a second-order pair function generated with Hartree-Fock orbitals [Fig. 12(b)].

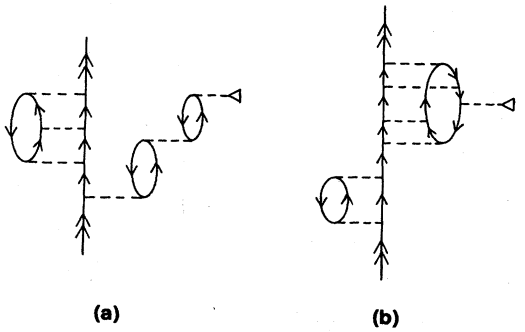

(a) (b)

FIG. 14. Examples of higher-order hyperfine diagrams, which are included when pair functions from higher iterations of the pair equation—together with iterated single-particle functions—are used to evaluate the core polarization (a) and the third-order diagrams (b).

grid, normally with $(x_{\min},\Delta x)=(-10,0.1)$, where $x_{\min}$ is the first value of $x=\ln r$, and Δx is the integration step. In Table I we have given the HF values for the ionization energy (or valence electron binding energy) as well as the HF and polarization values of the hyperfine parameters of the two states using this grid and with the two starting potentials mentioned. (The polarization of the core, with only s electrons, does not influence the orbital parameter.) In the same table we have also given the corresponding results after extrapolation to the grid $(-\infty,0)$. It can be seen that the small difference in the results obtained with the finite grid is almost entirely eliminated by the extrapolation. This shows that the choice of local starting potential has extremely small influence on the final results, which is a good indication of the numerical accuracy in this part of the calculation. As a further check we have also compared the two iterated HF results with that obtained in a direct and independent HF calculation in the SCF program. Also here, the agreement is very good after the grid extrapolation. (For the 2^2S state the HF solutions were not stable enough to allow for an accurate extrapolation.)

As mentioned, core-polarization calculations can be carried out either with the hyperfine or the electrostatic interaction as the perturbation[10] (see Figs. 4 and 5), and a comparison of the two results can give another indication about the numerical accuracy. As seen from Table I, the two approaches give slightly different results for the con-

TABLE I. Comparison between different numerical procedures to evaluate the HF values of the ionization energy and the HF and polarization values of the hyperfine parameters in the (a) 2^2S and (b) 2^2P states of the lithium atom.

(a) 2^2S

Grid	Starting pot.	Perturb.	Ionization energy	Hyperfine parameter HF	Polariz.
−10,0.1	OHFS (atom)	Hyp.	0.196 304 57	1.372 442	0.509 050
		Elec.			0.508 978
	OHFS (ion)	Hyp.	0.196 306 34	1.372 652	0.509 029
		Elec.			0.508 957
	HF		0.196 307 14		
Extrapol.	OHFS (atom)	Hyp.	0.196 304 33	1.372 218	0.509 136
		Elec.			0.509 137
	OHFS (ion)	Hyp.	0.196 304 31	1.372 214	0.509 137
		Elec.			0.509 139
	HF		0.196 304		

(b) 2^2P

Grid	Starting pot.	Perturb.	Ionization energy	Hyperfine parameter HF=orbital	Spin-dipole	Contact	Quadrupole
−10,0.1	OHFS atom	Hyp.	0.128 637 02	0.058 458 09	0.004 176 62	−0.151 4073	−0.006 937 46
		Elec.				−0.151 3860	
	OHFS (ion)	Hyp.	0.128 638 42	0.058 456 22	0.004 176 42	−0.151 4031	−0.006 937 30
		Elec.				−0.151 3820	
	HF		0.128 637 99	0.058 458 8			
Extrapol.	OHFS (atom)	Hyp.	0.128 636 72	0.058 456 37	0.004 176 37	−0.151 5106	−0.006 935 11
		Elec.				−0.151 4113	
	OHFS (ion)	Hyp.	0.128 636 77	0.058 456 39	0.004 176 36	−0.151 4106	−0.006 935 10
		Elec.				−0.151 4114	
	HF		0.128 636 72	0.058 456 33			

TABLE II. Effect of electron correlation upon the ion-core energy and ionization energy in the 2^2S and 2^2P states in successive iterations of pair functions and Brueckner orbitals.

Iteration	Ion-core energy	Ionization energy 2^2S	Ionization energy 2^2P
1	0.039 788	0.001 6365	0.001 3596
2	0.042 797	0.001 7958	0.001 5418
3	0.043 326	0.001 8248	0.001 5750
4	0.043 426	0.001 8313	0.001 5818
5	0.043 455	0.001 8331	0.001 5835
6	0.043 468	0.001 8337	0.001 5841
Extrapol.	0.043 475	0.001 8340	0.001 5843

TABLE IV. Effect of Brueckner orbitals upon the zeroth-order hyperfine parameters.

Iteration	2^2S	2^2P
1	0.047 991	0.003 6191
2	0.053 300	0.004 0626
3	0.054 334	0.004 1422
4	0.054 572	0.004 1591
5	0.054 637	0.004 1640
6	0.054 654	0.004 1660
Extrapolated	0.054 658	0.004 1667

tact parameters using a finite grid, but also this difference disappears after the grid extrapolation. As a result of this analysis we can conclude that the extrapolated values of the ionization energies and hyperfine parameters on this level are accurate to at least a few parts per million.

In the pair program we also use a logarithmic grid, in the present calculation from $x=-7.5$ to 3.0 with 41, 59, and 89 grid points. Extrapolation to eliminate the effect of the finite grid is made in the usual way. Here, the effect of the finite grid is much larger than in the self-consistent field and polarization calculations, due to the relatively coarse grid. In addition, the error is proportional to the second power of the integration step, due to the discontinuity in the electrostatic operator, compared to the fourth power in the SCF and POLAR routines.

In principle, there is no limitation on the l values in the pair excitations, and in order to avoid too many extrapolations we have in this calculation increased the maximum l value by one unit in each iteration cycle indicated in Fig. 3, starting with $l_{\max}=4$. This means that in the first iteration (step 4) the following pair functions are calculated:

$$1s^2 \rightarrow s^2, p^2, d^2, f^2, g^2 ,$$

$$1s\,2s \rightarrow s^2, p^2, d^2, f^2, g^2 ,$$

$$1s\,2p \rightarrow sp, ps, pd, pd, df, fd, fg, gf .$$

In the next iteration (step 8) the following pair excitations are added:

$$1s^2 \rightarrow h^2, \quad 1s\,2s \rightarrow h^2, \quad 1s\,2p \rightarrow gh, hg ,$$

and so on.

As a test of the goodness of the pair functions and the Brueckner orbitals in each iteration, we have evaluated the correlation energy of the ion core (depends only on the $1s^2$ pair) and the effect of the electron correlation upon the 2^2S and 2^2P ionization energies (which is equal to the difference between the HF and the Brueckner orbital energies). The results are shown in Table II. As an illustration of the grid-extrapolation procedure, we have in Table III shown the ion-core correlation energies obtained in the first four iterations, using three different grids and three different extrapolations. (41-59 and 59-89 represent quadratic extrapolations, eliminating the quadratic error, while 41-59-89 represents a fourth-order extrapolation.)

Table IV gives the effect on the zeroth-order hyperfine parameters of the use of Brueckner orbitals in successive iterations (see Figs. 8 and 9). Each iteration corresponds to one cycle, i.e., points 6—9, in the procedure described above. Table V gives the corresponding effects on the core polarization, i.e., effects of the kind illustrated in Figs. 11 and 14(a). Table VI, finally, gives the third-order hyperfine effects when pair functions and Brueckner orbitals are used in successive iterations [see Figs. 7, 13, and 14(b)].

The final results are collected in Tables VII and VIII, where they are compared with experimental results as well as with results of other accurate calculations. Our final results are corrected for relativistic effects and finite-nuclear-size effects by means of relativistic SCF (Ref. 35) and POLAR (Ref. 37) programs, using homogeneous nuclear charge density and pointlike nuclear moments. As can be seen from the tables, these effects are here only of the order of 0.1% or less and therefore of little significance for the present comparisons.

The uncertainties given for our theoretical results indi-

TABLE III. Ion-core correlation energy in different grids and different extrapolations. Last column represents a fourth-order extrapolation, eliminating the second- as well as fourth-order error due to the finite grid.

Iter.	41 pt.	59 pt.	89 pt.	41-59	59-89	41-59-89
1	0.041 349	0.040 495	0.040 087	0.039 721	0.039 774	0.039 788
2	0.044 234	0.043 455	0.043 078	0.042 749	0.042 787	0.042 797
3	0.044 813	0.044 007	0.043 616	0.043 275	0.043 316	0.043 326
4	0.044 931	0.044 116	0.043 720	0.043 377	0.043 416	0.043 426

TABLE V. Effect of Brueckner orbitals upon the core polarization.

Iteration	2^2S	2^2P Spin-dipole	2^2P Contact	2^2P Quadrupole
1	0.015 832	0.000 3337	−0.010 253	−0.000 2412
2	0.017 604	0.000 3763	−0.011 578	−0.000 2714
3	0.017 893	0.000 3834	−0.011 822	−0.000 2772
4	0.017 956	0.000 3851	−0.011 871	−0.000 2783
5	0.017 971	0.000 3855	−0.011 884	−0.000 2786
6	0.017 976	0.000 3856	−0.011 889	−0.000 2788
Extrapolated	0.017 977	0.000 3856	−0.011 891	−0.000 2788

TABLE VI. "Third-order" hyperfine effects, evaluated with pair functions in successive iterations. The single-particle functions are in all cases iterated to self-consistency.

Iteration	2^2S	Orbital	2^2P Spin-dipole	2^2P Contact	2^2P Quadrupole
1	−0.014 085	0.000 3179	0.000 0747	0.015 541	0.001 0194
2	−0.010 945	0.000 4236	0.000 1575	0.015 941	0.001 2094
3	−0.009 656	0.000 4455	0.000 1728	0.016 112	0.001 2460
4	−0.009 264	0.000 4499	0.000 1755	0.016 132	0.001 2540
5	−0.009 176	0.000 4509	0.000 1767	0.016 100	0.001 2552
6	−0.009 162	0.000 4511	0.000 1772	0.016 079	0.001 2554
Extrapolated	−0.009 158	0.000 4512	0.000 1774	0.016 079	0.001 2555

TABLE VII. Ion-core energy and ionization energies.

	Ion-core energy	Ionization energy 2^2S	Ionization energy 2^2P
Hartree-Fock	−7.236 415(2)	0.196 304(1)	0.128 637(1)
Pair correlation	−0.043 475(10)	0.001 834(2)	0.001 584(2)
Relativistic correction		0.000 016	0.000 000
Total	−7.279 890(10)	0.198 154(3)	0.130 221(3)
Experimental	−7.279 913[f]	0.198 159[g]	0.130 246[g]
Weiss[a]		0.197 19[h]	0.128 47[h]
Larsson *et al.*[b]		0.198 11[h]	0.130 08[h]
Sims *et al.*[c]		0.198 11[h]	
Nesbet[d]		0.196 94[h]	
Chang *et al.*[e]		0.198(2)	

[a]Reference 41.
[b]Reference 42.
[c]Reference 43.
[d]Reference 44.
[e]Reference 45.
[f]This is the "nonrelativistic" energy calculated by Pekeris (Ref. 46).
[g]Reference 47.
[h]These values are calculated from the total energies, using the nonrelativistic energy of the ion core.

cate only the uncertainty in the numerical procedure, including the extrapolations. No estimate has been made of the uncertainty in the relativistic and finite-nuclear-size corrections, nor of remaining correlation effects. The latter will be discussed in Sec. IV.

IV. DISCUSSION

The core of the lithium ion is heliumlike, and here a pair-correlation approach should, in principle, be exact. As can be seen from Table VII, our value for the ion-core

TABLE VIII. Hyperfine parameters for the lithium atom (in a.u.).

	2^2S		2^2P		
	Contact	Orbital	Spin-dipole	Contact	Quadrupole
Hartree-Fock (ion)	1.372 22(1)	0.058 456(1)	0.058 456(1)	0	0.058 456(1)
Core polarization	0.509 14(1)	0	0.004 176(1)	−0.151 41(1)	−0.006 935(1)
Brueckner orbitals	0.054 66(2)	0.004 167(2)	0.004 167(2)	0	0.004 167(2)
Effect of Brueckner orb. on core polarization	0.017 98(3)	0	0.000 386(2)	−0.011 89(2)	−0.000 279(2)
Third-order diagrams	−0.009 16(3)	0.000 451(2)	0.000 177(2)	0.016 08(10)	0.001 256(2)
Relativistic nuclear size correction	0.0011	0.000 004	0.000 018	−0.00007	−0.000 003
Total	1.9459(2)	0.063 08(1)	0.067 38(1)	−0.1473(2)	0.056 66(1)
Experimental[a,b,c]	1.9397	0.0627(3)	0.0678(4)	−0.1427(3)	
Larsson *et al.*[d]	1.937	0.0634	0.0671	−0.1441	0.0504
Nesbet[e]	1.9148	0.063 22	0.067 62	−0.1431	0.057 06
Chang and Das *et al.*[f]	1.927	0.062 81	0.068 59	−0.1386	0.0486
Hibbert *et al.*[g]	2.009	0.0625	0.0690	−0.1419	0.061 75
Garpman *et al.*[h]	1.939	0.062 62	0.066 60	−0.1380	0.056 34

[a]Reference 49.
[b]Reference 50.
[c]The experimental values are obtained using a nuclear magnetic moment of 3.2564 nuclear magnetons (Ref. 51) and a conversion factor of 95.4048 to transform from MHz to atomic units (with the nuclear moment in nuclear magnetons). This conversion factor also contains a correction for the reduced mass, corresponding to a nuclear mass of 6.5 amu.
[d]Reference 42.
[e]Reference 44.
[f]Reference 45.
[g]Reference 48.
[h]Reference 10(b).

energy agrees with the very accurate (nonrelativistic) value calculated by Pekeris[46] almost within our estimated numerical uncertainty. The correlation part of this energy seems to be accurate to at least one part in a thousand.

Also, the ionization energies (valence-electron binding energies) agree very well with the experimental data, although the deviation for the 2^2P state is outside the numerical uncertainty. (The almost perfect agreement for the 2^2S state is probably partly fortuitous.) The deviation for the 2^2P state is of the order of one percent of the correlation contribution, which is quite a reasonable three-body effect. This indicates strongly that the two-body part is, in fact, obtained very accurately in this procedure—at least with an accuracy on the percent level.

In Table VII we have also given the results of some other accurate energy calculations. The calculations of Weiss[41] are of configuration-interaction (CI) type, with about 45 configurations, while those of Larsson *et al.*[42] and of Sims *et al.*[43] are of Hylleraas type, with the interelectronic distances explicitly in the wave function. Nesbet[44] has used so-called Bethe-Goldstone equations, which are closely related to the pair equations used in the present work. The calculation of Nesbet, however, is performed in the independent electron-pair approximation (IEPA), which implies that there is no coupling between different pair excitations in different orders. In addition, only excitations with $l \leq 3$ are included. Chang *et al.*,[45] finally, use a diagrammatic approach, similar to that used in the present work, but only effects to third order are considered.

From the comparison in Table VII it can be concluded that—as far as the total energy and ionization energies are concerned—only the extensive Hylleraas-variational calculations of Larsson *et al.* and of Sims *et al.* have an accuracy comparable with that of the present work.

The hyperfine parameters obtained in the present work agree with the experimental results within the combined numerical and experimental uncertainties, except for the ^2S and ^2P contact parameters (see Table VIII). In Table IX the corresponding magnetic dipole interaction or A factors are given, and there it can be seen that there is a small, but significant, deviation between the theoretical and experimental results in all cases. It is interesting to note, however, that the agreement is almost perfect for the

TABLE IX. Magnetic dipole interaction constants divided by the nuclear g factor (A/g_I, in MHz per nuclear magneton). These results are obtained from the data in Table VIII. The uncertainty in the nuclear magnetic moment is *not* considered.

State	Hartree-Fock	Present work	Expt.
2^2S	130.92	185.65(2)	185.06(1)
$2^2P_{1/2}$	14.87	21.28(1)	21.15(2)
$2^2P_{3/2}$	2.97	−1.53(1)	−1.41(1)
$^2P_{1/2}+{}^2P_{3/2}$	17.85	19.75(2)	19.74(2)

sum of the two A factors of the ^2P state, which is independent of the contact parameter.[35(b)] Two important conclusions can be drawn from this comparison. First, one can conclude that it is quite unlikely that the discrepancy is due to errors in the analysis of the experimental data or in the nuclear magnetic moment used in the evaluation of the A/g_I values. Second, the comparison indicates strongly that our orbital and spin-dipole parameters are quite accurate—most likely more accurate than the corresponding experimental values—and that the discrepancy is due to a slight inaccuracy in our theoretical contact parameters. Possible reasons for this inaccuracy will be discussed below.

At first sight, the errors in the contact parameters may seem surprisingly large, considering the high accuracy obtained in the other cases. It should be observed, however, that the effect of the perturbation, i.e., the deviation from the Hartree-Fock value, is particularly large for the contact parameters—100% for the ^2P state and about 30% for the ^2S state. This should be compared with about 10% for the orbital and spin-dipole parameters and about 1% for the ionization energies. Therefore, compared with the leading perturbations, the residual errors are not considerably larger for the contact parameters than for the other quantities—about 1% for the ^2S and about 3% for the ^2P contact parameter. As mentioned previously, three-body contributions of this order of magnitude are not unreasonable.

It should be observed, however—as mentioned briefly in Sec, II C—that there are also certain two-body or pair-correlation effects missing in the present calculation. These are of two types, illustrated in Figs. 15(a) and 15(b). Diagram 15(a) represents a coupling between single and double excitations, which is not included. (This particular diagram can be regarded as a Brueckner-orbital modification of a *virtual* orbital.) In order to include this type of effect in our procedure, it is necessary to generate new pair functions with SPF as input (instead of core and valence orbitals). This is quite feasible but has not yet been done. In order to include the second missing pair-correlation effect, illustrated in Fig. 15(b), still another class of pair functions is needed, this time with a passive valence orbital. Both these effects appear for the first time in the fourth order of the perturbation expansion. Considering the energy denominators, however, one can expect the first effect, Fig. 15(a), to dominate. In diagrams of this kind there is only one double core excitation, and it is therefore not unreasonable to expect this effect to represent a few percent of the entire perturbation effect. This can be compared with the effect of using Brueckner orbitals upon the core polarization, which also enters in fourth order (see Fig. 11). This effect is for the ^2S parameter 3—4% and for the ^2P contact parameter about 8% of the polarization effect. This effect is dominated by the modification of the valence orbital [Fig. 11(a)], but the omitted pair-correlation effects should be comparable with the effect of the Brueckner-orbital modification of the core levels.

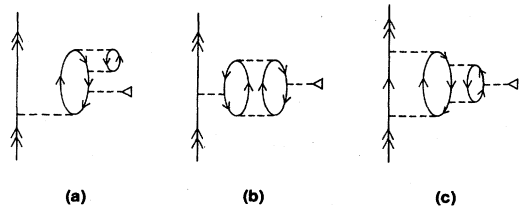

FIG. 15. Examples of correlation effects in the hyperfine interaction, which are *not* included in the present calculation. (a) represents a coupling between single and double excitations, which in this case can be regarded as a Brueckner-orbital modification of a *virtual* level [cf. Fig. 9(b), representing a corresponding modification of a *core* level]. (b) represents a double core excitation with an interaction with an unexcited valence electron. Effects of these two kinds *can* be included in an extended pair-correlation procedure. (c), on the other hand, represents a genuine three-body effect, which *cannot* be included in such a procedure.

Certain triple excitations are included in the present calculation, namely, such for which the denominators of the diagram can be "factorized.[9]" An example of such a diagram is shown in Fig. 14(a). Genuine three-body effects, on the other hand, which cannot be factorized in this way [see Fig. 15(c)], are *not* included in this calculation. We are convinced, however, that effects of this kind are much smaller than the missing pair-correlation effects, mentioned above.

Due to the violation of the exclusion principle, there are also nonzero diagrams with quadruple, etc., excitations, in spite of the fact that there are only three electrons in the system. The use of the coupled-cluster procedure [Eqs. (28) and (29)], however, ensures that the most important quadruple excitations are, in fact, included in the pair-correlation calculation.

From the arguments given here we can draw the conclusion that the remaining discrepancy between our contact parameters and the corresponding experimental values is most likely due to the omitted pair-correlation effects, illustrated in Fig. 15.

Our quadrupole parameter, given in Table VIII, should have an accuracy comparable with that of the orbital and spin-dipole parameters, i.e., of the order of 0.1%. This does not lead to any improved value of the quadrupole moment of the ^{7}Li nucleus, however, due to the experimental uncertainty in the interaction constant. Therefore, the best available moment is still that given by Orth *et al.*,[50]

$$Q(^7\mathrm{Li}) = -41(6)\ \mathrm{mb}\ .$$

In Table VIII we have also collected the results of some other accurate hyperfine calculations on the lithium atom. The calculations of Nesbet,[44] Larsson *et al.*,[42] and of Chang and Das *et al.*[45] are essentially the same as those discussed above. Hibbert's calculation[48] is of CI type, but including only excitations with $1 \leq 2$. The calculation of Garpman *et al.*,[10(b)] finally, is of the same kind as that reported on here but less complete. In particular, only first-order pair functions are used.

It can be seen from the comparison in Table VIII that the internal consistency of the theoretical calculations is reasonably good, particularly for the orbital and spin-

dipole parameters. In view of that, one finds the large spread in the quadrupole parameters surprising. The contact parameters agree generally well with the experimental results, but considering the large efforts made in the present work, it is obvious that the very good agreements obtained in some previous calculations must be largely fortuitous.

V. SUMMARY AND CONCLUSIONS

In this work we have described a procedure for many-body calculations on atomic systems, based on numerical solution of coupled inhomogeneous differential equations of one- and two-particle type. By solving this set of equations iteratively, it is possible to include effects of single and double excitations—i.e., core-polarization and pair-correlation effects—to essentially all orders of perturbation theory. The coupling between single and double excitations is found to be important and leads effectively to the use of Brueckner orbitals. By means of the coupled-cluster formalism, the most important quadrupole excitations are also included in the procedure.

This procedure is applied with high accuracy to the lowest ^2S and ^2P states of the lithium atom, where the total energy, ionization energy, and hyperfine structure is evaluated. Most of the experimental data are reproduced with very high accuracy, and from the analysis the following main conclusions can be drawn.

(a) The procedure of solving coupled one- and two-particle equations in the open-shell coupled-cluster formalism seems to be a very efficient way of calculating the pair-correlation effect in (small) atomic systems. For the lithium atom in its lowest states this procedure, as applied in this work, is capable of reproducing this effect with an accuracy of the order of one percent.

(b) The pair correlation, evaluated in the coupled-cluster formalism, represents a very good approximation to the entire correlation effect, at least for small systems. For the lithium atom genuine three-body effects, which cannot be obtained in a pair-correlation procedure, are, at most, of the order of one percent of the pair-correlation effect.

ACKNOWLEDGMENTS

The author wants to thank his co-workers, Jean-Louis Heully, Ann-Marie Pendrill, and Sten Salomonson for many stimulating discussions.

[1]K. A. Brueckner, Phys. Rev. **100**, 36 (1955).
[2]J. Goldstone, Proc. R. Soc. London, Ser. A **239**, 267 (1957).
[3](a) H. P. Kelly, Phys. Rev. **131**, 684 (1963); (b) Adv. Chem. Phys. **14**, 129 (1969).
[4]B. Brandow, Rev. Mod. Phys. **39**, 771 (1967).
[5]P. G. H. Sandars, Adv. Chem. Phys. **14**, 365 (1969).
[6](a) I. Lindgren, J. Phys. B **7**, 2441 (1974); (b) Int. J. Quant. Chem. Symp. **S12**, 33 (1978).
[7]G. Hose and U. Kaldor, Phys. Scr. **21**, 357 (1980).
[8]B. Jeziorski and H. Munkhorst, Phys. Rev. A **24**, 1668 (1981).
[9]I. Lindgren and J. Morrison, *Atomic Many-Body Theory,* Vol. 13 of *Springer Series in Chemical Physics* (Springer, Berlin, 1982).
[10](a) S. Garpman, I. Lindgren, J. Lindgren, and J. Morrison, Phys. Rev. A **11**, 758 (1975); (b) Z. Phys. A **276**, 167 (1976).
[11](a) I. Lindgren, J. Lindgren, and A.-M. Mårtensson, Z. Phys. A **279**, 111 (1976); (b) Phys. Rev. A **15**, 2123 (1977).
[12]I. Lindgren, Rep. Prog. Phys. **47**, 354 (1984).
[13]L. Holmgren, I. Lindgren, J. Morrison, and A.-M. Mårtensson, Z. Phys. A **276**, 179 (1976).
[14]I. Lindgren and A.-M. Mårtensson, Phys. Rev. A **26**, 3249 (1982).
[15]A.-M. Mårtensson, J. Phys. B **12**, 3995 (1979).
[16](a) I. Lindgren and S. Salomonson, Phys. Scr. **21**, 335 (1980); (b) J. Morrison and S. Salomonson, *ibid.* **21**, 343 (1980); (c) S. Salomonson, I. Lindgren, and A.-M. Mårtensson, *ibid.* **21**, 351 (1980).
[17]A.-M. Mårtensson and S. Salomonson, J. Phys. B **15**, 2115 (1982).
[18]E. Lindroth and A.-M. Mårtensson-Pendrill, Z. Phys. A **316**, 265 (1984).
[19]A.-M. Mårtensson, Phys. Scr. **21**, 293 (1980).
[20]A.-M. Mårtensson, E. M. Henley, and L. Wilets, Phys. Rev. A **24**, 308 (1981).
[21]S. Salomonson, Z. Phys. A **316**, 135 (1984).
[22]C. Bloch, Nucl. Phys. **6**, 329 (1958).
[23](a) V. Kvasnička, Czech. J. Phys. B **24**, 605 (1974); **27**, 599 (1977); (b) Adv. Chem. Phys. **36**, 345 (1977); (c) V. Kvasnička, V. Laurinc, and S. Biskupič, Phys. Rep. **90**, 159 (1982).
[24](a) J. Čížek, J. Chem. Phys. **45**, 4256 (1966); (b) Adv. Chem. Phys. **14**, 35 (1969).
[25](a) J. Paldus and J. Čížek, Adv. Quant. Chem. **9**, 105 (1975).
[26]It should be noted that the x coefficients in the operator (22) are not identical to—but rather linear combinations of—the coefficients of the operator (20).
[27]The terms "connected" and "disconnected" should not be confused with "linked" and "unlinked." An unlinked diagram has a disconnected part, which is *closed,* while a linked wave-operator diagram can be disconnected, provided all parts are *open.*
[28]R. M. Sternheimer, Phys. Rev. **80**, 102 (1950).
[29](a) A. Dalgarno, Proc. R. Soc. London **251**, 282 (1959); (b) Adv. Phys. **11**, 281 (1962).
[30]J. Morrison, J. Phys. B **6**, 2205 (1973).
[31]V. McKoy and N. W. Winter, J. Chem. Phys. **48**, 5514 (1968).
[32]P. O. Löwdin, J. Math. Phys. **3**, 1171 (1958).
[33]J. C. Slater, Phys. Rev. **81**, 385 (1950).
[34](a) I. Lindgren, Phys. Lett. **19**, 382 (1965); (b) Ark. Fys. **31**, 59 (1966).
[35](a) A. Rosén and I. Lindgren, Phys. Rev. **176**, 114 (1968); (b) I. Lindgren and A. Rosén, Case Stud. At. Phys. **4**, 93 (1974).
[36](a) J. Slater, T. M. Wilson, and J. H. Wood, Phys. Rev. **179**, 28 (1969); (b) T. M. Wilson, J. H. Wood, and J. C. Slater, Phys. Rev. A **2**, 620 (1970).
[37](a) J. L. Heully and A.-M. Mårtensson-Pendrill, Phys. Scr. **27**, 291 (1983); (b) Phys. Rev. A **27**, 3332 (1983).
[38]H. Lundberg, A.-M. Mårtensson, and S. Svanberg, J. Phys. B **10**, 1971 (1977).
[39]A.-M. Mårtensson-Pendrill and S. Salomonson, Phys. Rev. A **30**, 712 (1984).
[40]R. Latter, Phys. Rev. **99**, 510 (1955).
[41](a) A. W. Weiss, Phys. Rev. **132**, 1826 (1961); (b) Astrophys. J.

138, 1262 (1963).
[42](a) S. Larsson, Phys. Rev. **169**, 49 (1968); (b) T. Ahlenius and S. Larsson, Phys. Rev. A **8**, 1 (1973).
[43]J. S. Sims, S. A. Hagstrom, and P. R. Rumble, Jr., Phys. Rev. A **14**, 576 (1976).
[44](a) R. K. Nesbet, Phys. Rev. **155**, 56 (1967); (b) in *Proceedings of the International Colloquium on Magnetic Hyperfine Structure of Atoms and Molecules, Paris, 1966,* edited by R. Lefebvre and C. Moser (CNRS, Paris, 1967); (c) Phys. Rev. A **2**, 661 (1970).
[45](a) E. S. Chang, R. T. Pu, and T. P. Das, Phys. Rev. **174**, 1 (1968); (b) J. D. Lyons, R. T. Pu, and T. P. Das, *ibid.* **178**, 103 (1969).
[46]C. L. Pekeris, Phys. Rev. **112**, 1649 (1958).
[47](a) C. E. Moore, *Atomic Energy Levels,* Natl. Bur. Stand. (U.S.) Circ. No. 467 (U.S. GPO, Washington, D.C., 1952, 1971), Vol. I; (b) C.-J. Lorenzen and K. Niemax, Phys. Scr. **27**, 300 (1983).
[48]A. Hibbert, J. Phys. B **3**, 585 (1970).
[49]R. G. Schlecht and D. W. McColm, Phys. Rev. **142**, 11 (1966).
[50]H. Orth, H. Ackermann, and E. W. Otten, Z. Phys. A **273**, 221 (1975).
[51]C. M. Lederer and V. S. Shirley, *Table of Isotopes* (Wiley, New York, 1978).